Potential reuse of pre-treated municipal solid waste incineration fly ash through geopolymerization

Yahaya Yakubu[a,c*], Jun Zhou[b], Zhu Shu[b], Yassin Mbululo[a,d], Sakinatu Issaka[a], Zimo Sheng[b], Yu Zhao[b]

[a]School of Environmental Studies, China University of Geosciences (Wuhan), 388 Lumo Road, Wuhan, 430074, P. R. China.

[b]Engineering Research Center of Nano-Geomaterials of Ministry of Education, Faculty of Materials Science and Chemistry, China University of Geosciences, 388 Lumo Road, Wuhan, 430074, P. R. China.

[c]Zoomlion Ghana Limited, PMB 117, Madina-Accra, Ghana.

[d]Solomon Mahlangu College of Science and Education, Sokoine University of Agriculture, Morogoro, Tanzania

*Corresponding author's email: yinny76@hotmail.com

Abstract

This study confirmed that water washing pre-treatment is an effective way of reducing toxic metals and chloride in municipal solid waste incineration fly ash, and for increasing its quantity in various mixtures. It applied only pre-treated municipal solid waste incineration fly ash in a

geopolymer process, which produced a compressive strength of 4.67 MPa after 28 days of curing under ambient conditions, whilst a sample made up of 75 % of the same fly ash produced the highest compressive strength (4.68 MPa) using the same study conditions. Nevertheless, all the samples yielded high compressive strength after 28 days of curing, which met the 1989 USEPA unconfined compressive strength test (0.34 MPa / 50 psi), and the 2011 toxicity characteristic leaching procedure standards. Also, the sample with only FA (FAG100) possessed superior solidification/stabilization ability of almost all the toxic metals understudied when compared with the rest of the samples. Analysis of the physical properties of the samples revealed that the content of FA increased with the compressive strength of all the samples studied. Which suggests that the amount of metakaolin used probably had a retarding effect on the compressive strength.

Keywords: Fly ash; Potential reuse, Solidification/Stabilization; Toxic metal; Hazardous waste

1. Introduction

The gas purification process of municipal solid waste incineration (MSWI) facilities produce large amounts of fly ash (FA), which has harmful effects on public health and the environment, due to presence of toxic metal pollutants. Thus, treatment of the FA before reuse and/or disposal

is of great significance. Washing pre-treatment of MSWI FA with water is a suitable procedure for improving quality and increasing its quantity in cementitious mixtures. But it comes with extra costs associated with the construction, operation, and management of the washing plant and wastewater treatment units. Pre-treatment has been used in several studies to reduce leachable contents of incineration ash for reuse or safe disposal [1–17].

Wastewater generated during the washing process is a hydrosaline solution, which usually contains high concentration of toxic metals, alkali chlorides and sulphates that may cause serious pollution to the environment and pose public health risks. However, these salts can be recycled as resources instead of been discharged [1]. Chen et al. [3] suggest reuse of discharged wastewater through concentration by evaporation if the technology is applied to industrialized mass production. Nevertheless, disposal of sludge generated from MSWI FA washing process requires an initial treatment to lower the pH and ionic concentrations of cadmium, aluminium, zinc, and lead. Reduction in sulphate concentration is also necessary when wastewater is to be discharged into surface water. When sulphate reduction is not required, the wastewater can be successfully treated by decreasing the pH to 7.6 [18].

The term geopolymer is used to illustrate a number of synthetic alumino-silicate materials, which have potential application in a number of fields, basically as a substitution for ordinary Portland cement and for ceramic applications. There are two main components of geopolymers; alkaline liquids and the source materials. The source materials for geopolymers should be rich in aluminium (Al) and silicon (Si). Silica and alumina sources or any pozzolanic compounds that readily dissolve in alkaline media might be applied as sources of precursor species. These sources can be natural minerals such as clays or kaolinite. Secondary products such as slag, silica fume, fly ash, red mud, rice husk ash and others are applied as source materials. The source of selecting materials for synthesizing geopolymers hinges mainly on factors such as cost, availability, type of application, and demand by final users. Different reagents such as potassium hydroxide, sodium hydroxide, potassium silicate, sodium silicate, metakaolinite, blast furnace slag, and kaolinite have been used. Normally, geopolymers produce high compressive strength within 28 days and also result in better solidification/stabilization (S/S) of toxic metals [19].

Geopolymerization is both an emerging and promissory technique for the application of by-products, and more importantly for S/S of toxic metals in hazardous waste [20,21]. It also serves as a cost effective solution to numerous challenges where treatment of hazardous residues should be carried out before storage. Products made from this process are environmentally safe, and require only modest amount of energy to produce. Besides, the CO_2 emission resulting from this process is reduced by up to about 80 %, when compared with that of ordinary Portland cement production. The polymeric structure of Al–O–Si (Aluminum-Oxygen-Silicon) formed during the process constitutes the main structure of the geopolymer. The rate of this process is influenced by many factors. The rate of pozzolanic reactions are fast-tracked by FA/kaolinite ratio, initial solids content, water content, alkali concentration, silicate and aluminate ratio, curing temperature, pH, and the type of activators used [22–24]. Also, it has been confirmed that curing time and curing temperature significantly impact the compressive strength of geopolymers [25].

Furthermore, in a study carried out on S/S of MSWI FA containing Pb, Cd, Cr, Zn, and Ba by Luna Galiano et al. (2011) through the process of geopolymerization, compressive strength values were obtained in the range of 1 to 9 MPa after 7 and 28 days. The authors further observed that the concentration of toxic metals that leached from the S/S products were strongly dependent on pH, which indicate that the leachate pH was the most significant factor for the immobilization of toxic metals as suggested Yahaya et al. [27-28].

A study by [29] on the use of metakaolin to stabilize sewage sludge ash and MSWI FA in cement-based materials, shows that, environmental and practical performance of prepared mortars did not change important properties after the addition of residues. Moreover, the use of metakaolin resulted in a significant reduction of the toxic metals released from binder matrix and soluble fractions. Shiota et al. [30] also synthesized a solid product from mixtures of raw materials such as MSWI FA, aqueous sodium hydroxide, sodium silicate solution, and dehydrated pyrophyllite. After curing for 24 hours at 105 °C, they realized that their final product decreased the leaching of Pb, and its concentration in the leachate was 9.7×10^{-4} mg/L using the TCLP, and 7.0×10^{-3} mg/L using the Japanese leaching test, which satisfied the respective test criteria, resulting in successful stabilization of Pb in the solid. Also, the final product achieved a compressive strength of 2 MPa and comprised mostly of crystalline phases.

Zheng et al. [31] used the partial charge model to analyse ion reactions that take place in geopolymerization, by investigating the effects of FA type and activator dosage. Their investigation yielded a geopolymer type with maximum strength using an intermediary alkaline quantity. It was further realized that aluminate or silicate if incorporated into the activator they can enhance the immobilization efficiency and strength. Nevertheless, among these two, aluminate yielded the best performance.

A further study on the resistance to alkali and acid by metakaolin-MSWI FA based geopolymer using S/S has been carried out and reported by Jin et al. [31]. The final product yielded the lowest compressive strength of 36.1 MPa after leaching with 2 L acid rain at pH of 3.0, and 40.0 MPa after immersion in aqueous alkali for 30 days. Also, the leachate concentration of certain toxic metals (Cu, Cd, Cr, Hg, Pb, and Zn) from the MSWI FA decreased significantly with values ranging from 0.003 mg/L to 0.292, after the geopolymerization process. In addition, X-ray diffraction analyses of the samples did not produce a new crystalline phase when the MSWI FA was present. Furthermore, the scanning electron microscope (SEM) results confirmed that the metakaolin-MSWI FA based product offered a more closely layered structure, thus preventing toxic metals from leaching out [31,32] of the nano-modified composite geopolymers. This study is one of a series aimed at identifying the optimum methodology for large scale potential reuse of pre-treated MSWI FA as a sustainable alternative to landfill disposal. As a result it understudies how washing pre-treatment and the geopolymer process can further improve its physical and chemical characteristics for industrial application.

2. Materials and methods

The FA sample used in this study was obtained from Xinghuo waste incineration power plant in Wuhan City, Hubei Province, P. R. China. Gas purification technology of the incineration plant is done by firstly injecting hydrated lime ($Ca(OH)_2$) to neutralize the harmful acid gas, after which the gas is channelled through bag filters to intercept dust, acid gas neutralization products, residual hydrated lime, and so on.

2.1 Pre-treatment and analysis

The moisture content of the raw FA was determined by subtracting its final weight from the initial weight after drying a certain quantity in an oven at 105 °C for 24 hours. The loss on ignition (LOI) for the raw and washed FA samples was also determined by subtracting their final weights from the initial weights, after gradually heating specific amounts of the samples from room temperature to 750 °C and allowing them to cool down gradually to room temperature again. Pre-treatment of the MSWI FA was carried out by subjecting it to a two stage washing with distilled water, using a liquid/solid (L/S) ratio of 10 for 15 minutes, and stirring speed of about 30 revolutions per minute (rpm). After washing, the FA was filtered and dried at 105 °C for 24 hours, before laboratory tests were conducted it: thus, used in the FA geopolymer (FAG) process and other analysis.

2.2 XRF and XRD analyses

The chemical composition of the FA was determined by X-ray fluorescence (XRF, AXIOSmAX, PANalytical B. V.), whilst the mineral phases were determined by X-ray powder diffraction (XRD, D8-FOCUS, Bruker AXS).

The toxicity characteristic leaching procedure (TCLP) test was conducted according to the USEPA method 1311 to establish the concentration of the toxic metals. The pre-treated sample was sieved with a 0.45 mm sieve in order to obtain the same particles size used for the FAG samples, before it was used in the leaching test. The extraction liquid, with a pH value of 2.88 was prepared by dissolving 5.7 mL of glacial acetic acid in 1 L of deionized water. A certain amount of the extraction liquid was added to a polyethylene (PE) bottle containing the FA sample, with an L/S ratio of 20:1, followed by a rolling-over process at 30 rpm for 20 hours on an oscillator. The leachates from the samples (raw FA and washed FA) was filtered using syringes and filters with effective pore size of 220 nm and analysed by ICP-MS (Elan DRC-e, PerkinElmer).

2.3 Sample preparation

This study is part of a series of laboratory analyses of a FA sample collected from an incinerator in Wuhan, China [28]. It involved preparing geopolymer samples (FAG samples) by using sieved pre-treated FA, metakaolin, an activator made of Na_2SiO_3 (water glass), and distilled

water. The water glass used in this work was supplied by Zhongfa Water Glass Factory in Foshan, China. The alkali activator solution was prepared by dissolving solid sodium hydroxide (99.2 % NaOH analysis reagent purity) in the industrial water glass of a mix composition of 26.0 % SiO_2, 8.2 % Na_2O, and 65.6 % of H_2O (silica molecular modulus, Ms. (SiO_2/Na_2O = 3.2). The alkali activator solution was prepared 24 hours prior to the preparation of geopolymer samples under ambient conditions.

The quantity of FA used ranged from 55 % to 100 %, with the rest of the solid material made up of metakaolin (MK). The amount of activator used for each sample equalled the quantity of the FA in the sample, whilst the level of water equalled the quantity of the FA plus 10 g (= sample FA + 10 g) for samples incorporating MK. The amount of water used for the sample with only FA (FAG100) was equal to 60 % of the weight of the FA. The sample pastes were then cast into 3.2 cm x 3.2 cm x 3.2 cm moulds and cured under room conditions for 28 days, before analysing their compressive strength, toxic metal leachability, density, and mineral phases. Table 1 presents the quantities of FA, metakaolin, activator, and water used for each batch of the moulds during the geopolymer process.

Table 1 Materials used for FAG samples

Sample code	FA (g)	Metakaolin (g)	Activator (g)	Water (g)
FA100	60	-	60	36
FAG75	45	15	45	55
FAG70	42	18	42	52
FAG65	39	21	39	49
FAG60	36	24	36	46
FAG55	33	27	33	43

'-' means not used

2.4 Test methods for FAG samples

2.4.1 Leaching test

The toxicity characteristic leaching procedure (TCLP) test was conducted according to the USEPA method 1311. The crushed, ground and sieved FAG samples were used in the leaching

tests. The extraction liquid, with a pH value of 2.88 was prepared by dissolving 5.7 mL of glacial acetic acid in 1 L of deionized water. A certain amount of the extraction liquid was added to a polyethylene (PE) bottle containing the samples, with an L/S ratio of 20:1, followed by a rolling-over process at 30 rpm for 20 hours on oscillators. The leachate from the samples were filtered by using syringes and filters with effective pore size of 220 nm and analysed by ICP-MS (Elan DRC-e, PerkinElmer).

2.4.2 Property characterization

Compressive strength of the samples was measured according to the Chinese Standard (GB/T 17671-1999) on a WE-50 universal testing machine (Shandong Jinan Testing Machine Factory, China), by averaging from three bricks for each composition. The mineral phases of the samples were determined by XRD (D-FOCUS, Bruker AXS), with step scanning in the 2θ range from 5 ° to 70 ° at a rate of 4 °/min using Cu Kα radiation and Ni filter at a generator voltage of 40 kV and a current of 40 mA.

3. Results and discussions

3.1 Characterization of fly ash

The leachate pH of the sample FA after washing was 11.9 and 12.4 for the first and second washing, respectively, whiles that of the washed FA after drying was 12.3. The moisture content of the raw FA was 5.31 %, whilst the LOI was 16.67 % and 15.33 % for the raw and washed FA samples, respectively.

3.2 Chemical and mineralogical composition of raw FA

The chemical composition of untreated FA expressed as metal oxides or in their elemental state is presented in Table 2.

Table 2 Chemical composition of raw FA

Composition	SiO_2	Al_2O_3	Fe_2O_3	MgO	CaO	Na_2O	K_2O	MnO
Content (%)	64.72	14.83	5.33	1.92	2.27	1.70	2.78	0.001

Composition	TiO_2	P_2O_5	CO_2	Ba	Sr	Zr	Others
Content (%)	0.78	0.001	4.88	0.06	0.02	0.02	0.67

Table 2 presents the chemical composition of untreated FA expressed as metal oxides or in their elemental state. Silicon oxide (SiO_2) formed the major chemical component of the FA (64.72 %), followed by aluminium oxide (Al_2O_3) (14.83 %). These were followed by carbon dioxide (CO_2) (4.88 %), potassium oxide (K_2O) (2.78 %), calcium oxide (CaO) (2.27 %), magnesium oxide (MgO) (1.92 %), and sodium oxide (Na_2O) (1.70 %). The rest constituted less than 1 % each. The high level of silicon, aluminium, and calcium oxides, and the absence of chloride and sulphate contents in the raw FA makes it very suitable for use in the cement and concrete industries [33,34]. However, due to the presence of certain potentially toxic elements, such as manganese oxide (MnO), tin oxide (TiO_2), barium oxide (BaO), strontium (Sr), and zirconium (Zr)), the ash must be subjected to preliminary treatment before reuse and/or landfilling. With regards to the toxic metal oxides, Fe_2O_3 is the most concentrated toxic metal oxide (5.33 %), followed by manganese oxide (MnO) (1.92 %), titanium oxide (TiO_2) (0.78 %), and barium (Ba) (0.06 %). The rest constituted less than 0.06 % each.

Mineralogical composition of the FA is quite complex (Table 2). Lower peak intensities in the X-ray pattren (Fig. 1) of the raw FA show that most of the compounds in the ash are mainly in their amorphous state. The high number of lead oxide peaks in the X-ray of this FA indicates high level of Pb in the ash. Higher concentration of chlorides in the ash is observed through the higher peaks of the crystalline form of calcium chloride hydroxide (CaCl(OH)). The lower peak of halite (NaCl) confirms the presence of relatively small quantities of Na. Portlandite ($Ca(OH)_2$) occurred in relatively large amounts as compared with tin telluride (SnTn), which occurred in smaller amounts (Fig. 1).

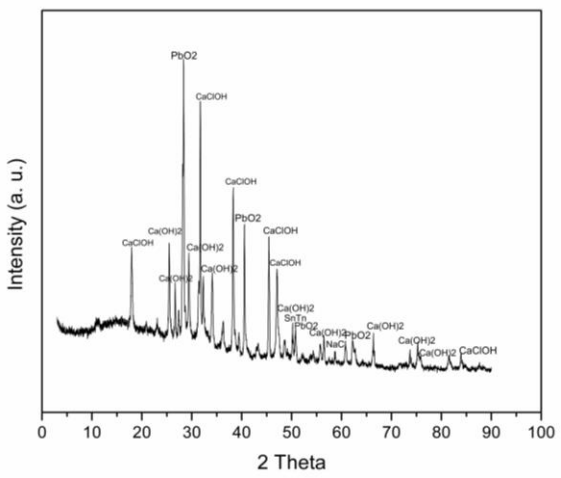

Fig. 1 X-ray pattern of raw FA. KCl - sylvite, SnTn - tin telluride, NaCl – halite, CaClOH – calcium chloride hydroxide, PbO_2 – lead oxide, $Ca(OH)_2$ – portlandite.

3.3 Chemical and mineralogical composition of washed FA

Regarding chemical composition of the washed FA (Table 3), carbon dioxide constituted the highest (37.67 %), followed by calcium oxide (32.30 %). These were followed by silicon oxide (13.20 %), aluminium oxide (5.66 %), magnesium oxide (2.97 %), sodium oxide (1.77 %), with the rest accounting for less 1 % each. With reference to the toxic metal oxides (Table 3), iron oxide is the most concentrated toxic metal oxide (2.32 %), followed by zinc (0.76 %), and lead (Pb) (0.19 %). The rest constituted less than 0.10 % each.

Table 3 Chemical composition of washed FA

Composition	SiO_2	Al_2O_3	Fe_2O_3	MgO	CaO	Na_2O	K_2O	MnO	P_2O_5
Content (%)	13.2	5.66	2.32	2.97	32.3	1.77	0.69	0.08	0.54
Composition			CO_2	Cr	Ni	Cu	Zn	Pb	Others
Content (%)			37.67	0.02	$4e^{-3}$	0.07	0.76	0.19	1.79

The chemical composition of the washed FA sample is also quite complex (Table 3). Lower peak intensities in the X-ray pattern (Fig. 2) for the washed FA show that most of the compounds in the ash are mainly in the amorphous form. High number of $CaCO_3$ peaks in the X- ray pattern of this FA indicate its high level in the ash. Higher concentrations of portlandite, quartz (SiO_2) and anhydrite ($CaSO_4$) are also observed in the ash through their high peaks. The peak of calcium

silicate hydroxide ($Ca_7Si_{16}O_{38}(OH)_2$) confirms its presence in a relatively small quantities (Fig. 2).

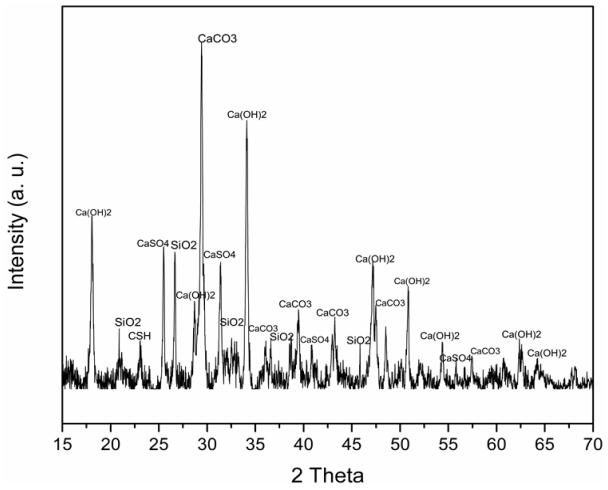

Fig. 2 X-ray pattern of washed FA. $CaSO_4$ - anhydrite, $CaCO_3$ – calcite, CSH – calcium silicate hydroxide ($Ca_7Si_{16}O_{38}(OH)_2$), SiO_2 - quartz, $Ca(OH)_2$ – portlandite.

The complete elimination of chlorides after washing proves the effectiveness of water washing pre-treatment. From the results of Figs. 1 and 2, it can be seen that all the chloride phases (sylvite, silicon chloride, and halite) were removed after the washing process, which is further corroborated by Wang et al. [14]. This therefore means that washing serves as a promising process of improving the quality of raw FA for further industrial application, since it is able to reduce the chloride content appreciably.

3.4 Pre-treated MSWI FA

Table 4 presents the comparison of toxic metals identified in the raw and washed ashes, and the USEPA-1311 TCLP regulatory limits.

Table 4 Comparison of toxic metals content and USEPA-1311 TCLP regulatory limits

Toxic metal	Raw FA (mg/L)	Washed FA (mg/L)	USEPA 1311 TCLP regulatory limit (mg/L)
Cr	136.74	1.90	50
Co	99.81	0.04	-
Ni	45.79	0.86	-
Cd	172.08	0.01	10
Cu	499.90	0.18	250
Zn	6430.31	3.30	-

'-' not available at the time of this study.

As it can been observed from Table 4, all the toxic metals in the raw FA sample exceeded the three available standards. Chromium (Cr) exceeded its limit by almost three times (136.74 mg/L), Cadmium (Cd) by more than seventeen times (172.08), whiles copper (Cu) is almost two times higher (499.90 mg/L). This makes the sample toxic under the USEPA-1311 TCLP classification, thereby requiring pre-treatment and proper handling.

However, after the washing pre-treatment the concentration of the toxic metals identified in this study reduced drastically, below their regulatory limits (Table 4), thereby making the FA compliant with regulatory requirements. It is worth mentioning that the washing process almost removed or immobilized all the contents of the leachable toxic metals identified in the raw FA. More than 98 % of each toxic metal was successfully removed or immobilized (Table 4). The washing process was excellent in removing or immobilizing Cd (99.99 %) and very good at the rest. About 99.96 % of Cu was successfully eliminated or immobilized, 99.96 % of cobalt (Co), 99.95 % of Zn, 98.61 % of Cr, and 98.12 % of nickel (Ni).

3.5 Chemical composition of leachate from pre-treatment

Table 5 presents a comparison of the toxic metals composition of the leachate from the washing process, the USEPA-1311 TCLP, and the China (GB 16889-2008) regulatory limits. It can be

seen from the results that the leachate complies with both regulatory limits and can be discharged without further treatment in both circumstances.

Table 5 Comparison of toxic metals in leachate and regulatory limits

Toxic metal	Leachate (mg/L)	USEPA-1311 regulatory limit (mg/L)	China (GB 16889-2008) (mg/L)
Cr	0.044	2	-
Co	0.003	-	-
Ni	0.052	-	0.5
Cu	0.018	3	40
Zn	0.091	5	100

'-' means not available at the time of this study.

From Table 5 Ni and Cu are far less than their respective GB 16889-2008 limit by more than nine times and two thousand times, respectively, whilst Zn was almost one thousand one hundred times less. Also, using the USEPA limits, Cu was almost one hundred and sixty seven times less, Zn was more than fifty four times less, and Cr was more than forty five times less (Table 5).

3.6 Potential reuse of pre-treated FA through geopolymerization

3.6.1 Evaluation of chemical and mineralogical characteristics

Table 6 presents the concentration of toxic metals in the samples prepared with washed FA through the geopolymer process (FAG samples). The pH of the mixture of crushed samples (< 1 mm size) and extraction solution was determined in order to find out its effect(s) on the leachability of toxic metals among the FAG samples.

From the results in Table 6, it appears the toxic metals leachability generally decreased as pH and FA content increased, even though most of the pH values for the samples are so close to

each other. This is further corroborated by Yahaya et al. [27], who concluded from their study on effects of pH dynamics on S/S of MSWI FA, and recommended a pH range of 5 to 11 for the management of MSWI FA. Therefore, this suggests that it is because the pH values are within the recommended range (5 to 11) that is why the FAG samples have been so effective in S/S of all the toxic metals.

Table 6: ICP results of FAG samples

		Cr	Mn	Co	Ni	Cu	Zn	Cd	Pb
Sample	pH	mg/L							
FAG100	7.2	7.10	0.41	0.07	0.38	0.78	0.45	0.20	0.22
FAG75	5.8	6.58	1.00	0.09	0.43	1.26	3.22	0.56	1.50
FAG70	5.7	5.94	1.87	0.12	0.42	2.12	18.94	1.55	2.34
FAG65	5.6	5.94	3.54	0.18	0.53	3.54	44.00	2.96	2.28
FAG60	5.6	5.70	4.84	0.22	0.52	6.10	<LOD	5.20	3.80
FAG55	5.7	6.06	5.70	0.25	0.61	6.22	<LOD	5.38	3.44

'<LOD' - less than limit of detection.

From Table 6 the highest amount of Cr leached out of FAG100 (7.1 mg/L) at pH of 7.2, whilst the least amount leached out of FAG60 (5.7 mg/L) at pH of 5.6. FAG70 and FAG65 leached the same amount of Cr (5.94 mg/L) at pH of 5.7 and 5.6, respectively. With regards to Mn and Co, their leachability increased as the amount of FA in the samples decreased, whilst FAG100 leached the least amount of 0.41 mg/L (Table 6). Moreover, the highest amount of Mn (5.70 mg/L) leached out of FAG55. The highest amount of Co leached in FAG55 (0.07 mg/L), whilst the lowest leached in FAG100 (0.07 mg/L). Ni leachability is highest in FAG55 (0.61 mg/L), and lowest in FAG100 (0.38 mg/L). The toxic metals leachability trend for Cu, Cd, Zn, and Pb are also very similar to that of Mn and Co. Their leachability generally decreased as amount of FA in the samples increased. The least amount of Cu (0.78 mg/L) leached out of FAG100, whiles the highest leached out of FAG55 (6.22 mg/L). Maximum leachability of Zn occurred in FAG65 (44.00 mg/L), whilst the minimum occurred in FAG100 (0.45 mg/L). However, its leachability was not detected in FAG60 and FAG55, thereby making these samples excellent for

it S/S. The least amount of Cd (0.20 mg/L) leached out of FAG100, whilst the highest leached out of FAG55 (5.38 mg/L). With reference to Pb, it leached the highest amount in FAG60 (3.80 mg/L), and the least in FAG100 (0.22 mg/L).

A look at the X-ray patterns for all the FAG samples (Figs. 3 to 8) reveal the presence of most of the toxic metals identified in the ICP results of these samples (Cu, Pb, Zn, and Cd) (Table 6) and XRF results of the washed FA (Fe and Ba), with the exception of Cr (Table 3). Ni appeared in the X-ray patterns of FAG70 and FAG55 as nickel carbide (NiCx) (Figs. 5 and 8), whilst Cu appeared in the X-ray pattern of FAG70 as copper vanadium oxide (CuV_2O_6) (Fig. 5). Zn and Ba appeared in the X-ray pattern of FAG55 as barium zinc phosphate (Fig. 8), whilst Ba alone appeared in FAG100 as nagashimalite ($Ba_4(V^{+3}, Ti)_4ClSi_8B_2O_{27}(O, OH)_2$ (Fig. 3). Cd and Pb appeared in the X-ray pattern of FAG55 as cadmium lead oxide ($CdPbO_3$) (Fig. 8), whiles Pb alone occurred in the X-ray pattern of FAG65 as lead oxide (Pb_2O_3) (Fig. 6). Fe was identified as potassium iron fluoride (K_2FeF_5) in FAG65 (Fig. 6), whiles Cr was absent in all the X-ray patterns of the samples understudy.

Other toxic metals identified in the X-ray patterns include tungsten (W), titanium (Ti), bismuth (Bi), vanadium (V), yttrium (Y), and antimony (Sb).

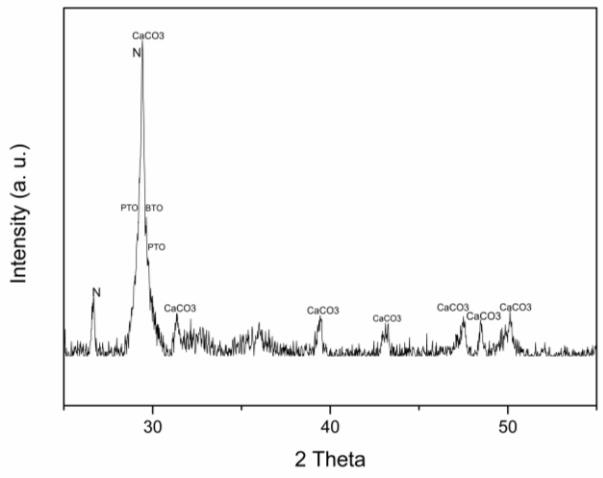

Fig. 3 X-ray pattern of FAG100. $CaCO_3$ – calcite, BTO – bismuth titanium oxide ($Bi_4Ti_3O_{12}$), YTO – yttrium titanium oxide (Y_2TiO_5), ASS – aluminium sodium selenide (AlNaSe2), N – nagashimalite ($Ba4(V+3, Ti)_4ClSi_8B_2O_{27}(O, OH)_2$, PTO – potassium titanium oxide ($K_2Ti_6O_{13}$).

Bi, Ti, and Y occurred in FAG100 as bismuth titanium oxide ($Bi_4Ti_3O_{12}$), and as yttrium titanium oxide (Y_2TiO_5) (Fig. 3). Also, V and Ti occurred in FAG100 as nagashimalite, whiles Ti alone appeared in FAG100 as potassium titanium oxide ($K_2Ti_6O_{13}$). Calcite was identified in the X-ray pattern of FAG100 as the dominant phase, followed by nagashimalite, potassium titanium oxide ($K_2Ti_6O_{13}$), and bismuth titanium oxide ($Bi_4Ti_3O_{12}$).

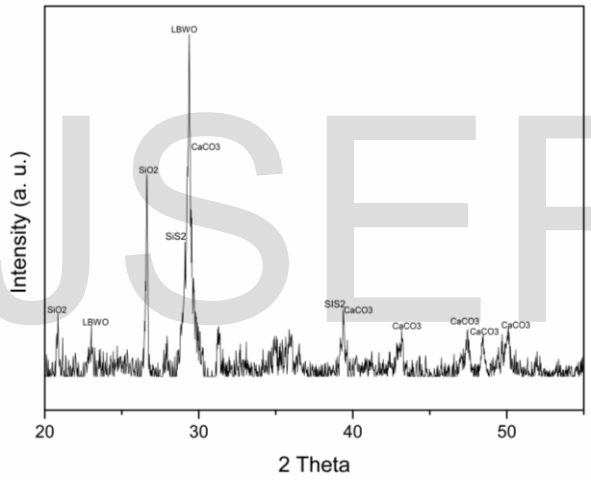

Fig. 4 X-ray pattern of FAG75. SiO_2 – quartz, $CaCO_3$ – calcite, SiS_2 – silicon sulphide, LBWO – lithium bismuth tungsten oxide ($LiBiW_2O_8$)

W and Bi occurred FAG75 as lithium bismuth tungsten (Fig. 4). The rest of the phases identified in FAG75 are quartz, calcite, and silicon sulphide. Lithium bismuth tungsten oxide ($LiBiW_2O_8$) occupied the highest peak, whiles most of the peaks were occupied by calcite, followed by quartz and silicon sulphide (Fig. 4).

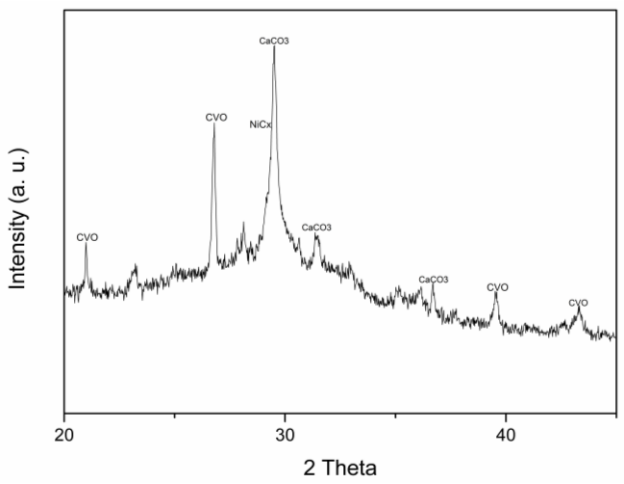

Fig. 5 X-ray pattern of FAG70. NiCx – nickel carbide, CVO – copper vanadium oxide (CuV_2O_6), $CaCO_3$ – calcite.

From Fig. 5 Ni occurred as nickel carbide (NiCx), whiles vanadium occurred as copper vanadium oxide (CuV_2O_6). The other phase identified in the X-ray pattern of FAG70 is calcite, which occupied the highest and most of the peaks. This was followed by copper vanadium oxide, and nickel carbide.

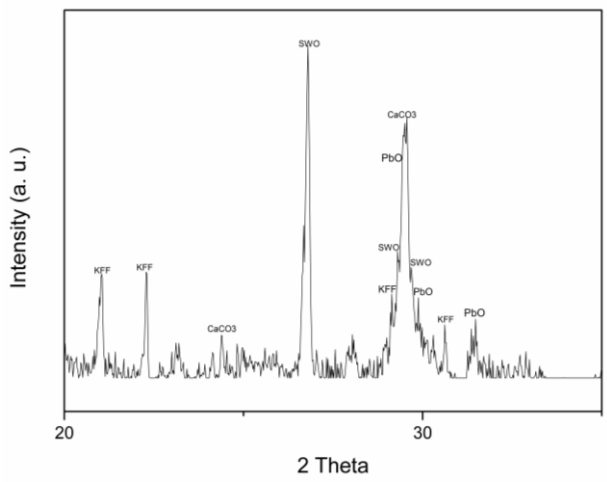

Fig. 6 X-ray pattern of FAG65. $CaCO_3$ – calcite, SWO – antimony tungsten oxide (Sb_2WO_6), PbO – lead oxide (Pb_2O_3), KFF – potassium iron fluoride (K_2FeF_5).

In the X-ray pattern of FAG65 antimony tungsten oxide (Sb_2WO_6) produced the highest peak, followed by calcite, lead oxide (Pb_2O_3), and potassium iron fluoride (K_2FeF_5). FAG65 had four toxic metal phases, notably antimony, tungsten, lead, and iron. This was expected because it is one of the samples that had the lowest pH (5.6) (Table 6).

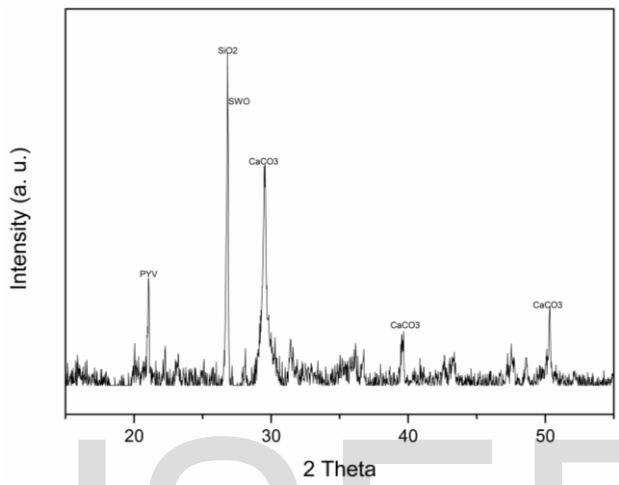

Fig. 7 X-ray pattern of FAG60. SiO2 – quartz, $CaCO_3$ – calcite, SWO – antimony tungsten oxide (Sb_2WO_6), PYV – potassium yttrium vanadate ($K_3Y(VO_4)_2$).

FAG60 also had four toxic metal phases in its X-ray pattern (Fig. 7) (antimony, tungsten, yttrium, and vanadium). This was because it also had the same pH as FAG65 (5.6), which resulted in more toxic metals leachability. However, quartz peaked high, followed by antimony tungsten oxide, calcite, and potassium yttrium vanadate ($K_3Y(VO_4)_2$). Even though quartz had the highest peak, calcite was the predominant phase in FAG60.

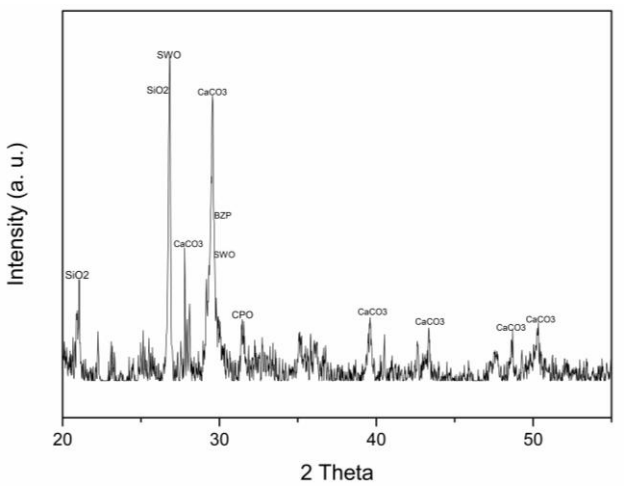

Fig. 8 X-ray pattern of FAG55. SiO2 – quartz, $CaCO_3$ – calcite, SWO – antimony tungsten oxide (Sb_2WO_6), CPO – cadmium lead oxide ($CdPbO_3$), BZP – barium zinc phosphate ($BaZnP_2O_7$).

Toxic metals such as antimony, tungsten, cadmium, lead, barium, and zinc were identified in the X-ray pattern of FAG55 (Fig. 8). Besides this sample having the highest number of toxic metal phases among all, it still had calcite as the predominant phase. Antimony tungsten had the highest peak, followed by quartz and calcite. Even though the samples produced through the geopolymer process had a number of toxic metal phases, the identified toxic metals are highly immobilized thereby resulting in effective S/S.

3.6.2 Evaluation of physical characteristics of FAG samples

The regression between density and compressive strength among the FAG samples was strong (r^2 = 0.864). Also, there is existence of an inverse relationship between the FA content and density. As the content of FA increased and the density decreased, the compressive strength of the samples increased. This suggest that the amount of metakaolin actually had a retarding effect on compressive strength development, since it was used as a replacement for the FA. This is so because the activator was used at a fixed ratio with the FA (1:1) for all the samples. The use of metakaolin therefore might not be necessary if the FA is properly pre-treated. But, quite interestingly, all the FAG samples passed the USEPA 1989 compressive test standard (Table 7).

Table 7 Physical characteristics of FAG samples

Sample	Density (g/cm^3)	Compressive strength (MPa)	Compared with the USEPA standards MPa/psi (0.34/>50)
FAG100	1.54	4.67	Passed
FAG75	1.60	4.68	Passed
FAG70	1.62	2.94	Passed
FAG65	1.68	2.22	Passed
FAG60	1.68	1.79	Passed
FAG55	1.70	1.79	Passed

The strong correlation trend observed among the FAG samples (Table 7) was due to the successful improvement in the cementitious quality of the FA through washing and the reaction that took place during the geopolymer process. Using a FA to activator (FA/activator) ratio of 1 resulted in the achievement of high strength material (Tables 1 and 7). It can be observed from Table 7 that compressive strength generally decreased with the quantity of FA used. This makes the process superior in terms of compressive strength development. The highest compressive strength was attained by FAG75 (4.68 MPa), followed by FAG100 (4.67 MPa). These were followed by FAG70 (2.94 MPa), FAG65 (2.22 MPa), FAG60 (1.79 MPa), and FAG55 (1.79 MPa) (Table 7). The difference between the compressive strengths for FAG100 and FAG75 (0.01 MPa) can be compromised, thereby making the best sample FAG100. Using the USEPA 1989 standard of 0.34 MPa, the compressive strength of the FAG samples is more than four times this recommended value. The compressive strength of FAG75 and FAG100 (4.68 MPa and 4.67 MPa, respectively) which were the highest among the samples is almost fourteen times the USEPA 1989 standard. That of FAG70 is almost nine times higher (2.94 MPa), FAG65 is almost seven times higher, whilst FAG55 is more five times the recommended value of 0.34 MPa.

4 Conclusion

The washing process has proved to be effective in reducing the chloride and toxic metals in MSWI FA, thereby increasing the quantity of FA that can be incorporated in cementitious mixtures. Applying 100 % of the pre-treated FA (FAG100) in the geopolymer process yielded a

28 days compressive strength of 4.67 MPa, which is almost equal to that of the highest among the samples which incorporated 75 % of the pre-treated FA (FAG75) and produced a 28 days compressive strength of 4.68 MPa. The difference between the two (FAG100 and FAG75) was almost negligible (~ 0.21 %). Nevertheless, all the samples produced high compressive strength after 28 days of curing which passed the USEPA 1989 standard criteria. Also, FAG100 had superior S/S ability for almost all the toxic metals understudy compared with rest of the samples. From the analysis of the physical characteristics of the FAG samples, it was clear that as the content of FA increased, density decreased, and compressive strength increased. Also, a decrease in the amount of FA generally resulted in an increase in the toxic metals concentration in all the samples. The relationship between FA content, density and compressive strength of the samples was very strong. However, there exist a strong correlation between the FA content and compressive strength: as the content of FA increased, the compressive strength generally increased.

Conflict of interest

All authors declare that they do not have any conflict of interest in this study. Also, this article does not contain any studies with human participants or animals.

Acknowledgement

The support of staff from Xinghuo waste incineration power plant in Wuhan City, Hubei Province, P. R. China for providing the FA sample and also taking the authors through the plant operations processes is appreciated.

Funding

The authors gratefully acknowledge the support of this research by the National Natural Science Foundation of China (41502030, 51502272), Science and Technology Department of Hubei Province of China (2017ACA091), the Zhejiang Provincial Natural Science Foundation of China (LQY18D020001) and the Open Foundation of Engineering Research Center of Nano-

Geomaterials of Ministry of Education of China (NGM2017KF008), the Chinese Scholarship Council (CSC), and the Government of Ghana (GoG).

Reference

[1] H. Tang, A. Erzat, Y. Liu, Recovery of soluble chloride salts from the wastewater generated during the washing process of municipal solid wastes incineration fly ash, Environ. Technol. (United Kingdom). 35 (2014) 2863–2869. doi:10.1080/09593330.2014.924568.

[2] R. Yang, W.P. Liao, P.H. Wu, Basic characteristics of leachate produced by various washing processes for MSWI ashes in Taiwan, J. Environ. Manage. 104 (2012) 67–76. doi:10.1016/j.jenvman.2012.03.008.

[3] X. Chen, Y. Bi, H. Zhang, J. Wang, Chlorides Removal and Control through Water-washing Process on MSWI Fly Ash, Procedia Environ. Sci. 31 (2016) 560–566. doi:10.1016/j.proenv.2016.02.086.

[4] F. Zhu, M. Takaoka, K. Oshita, N. Takeda, Comparison of two types of municipal solid waste incinerator fly ashes with different alkaline reagents in washing experiments, Waste Manag. 29 (2009) 259–264. doi:10.1016/j.wasman.2008.03.008.

[5] L. Reijnders, Disposal, uses and treatments of combustion ashes: A review, Resour. Conserv. Recycl. 43 (2005) 313–336. doi:10.1016/j.resconrec.2004.06.007.

[6] T.J. Xu, Y.P. Ting, Fungal bioleaching of incineration fly ash: Metal extraction and modeling growth kinetics, Enzyme Microb. Technol. 44 (2009) 323–328. doi:10.1016/j.enzmictec.2009.01.006.

[7] Y. Jiang, B. Xi, X. Li, L. Zhang, Z. Wei, Effect of water-extraction on characteristics of melting and solidification of fly ash from municipal solid waste incinerator, J. Hazard. Mater. 161 (2009) 871–877. doi:10.1016/j.jhazmat.2008.04.033.

[8] Q. Wang, J. Yang, Q. Wang, T. Wu, Effects of water-washing pretreatment on bioleaching of heavy metals from municipal solid waste incinerator fly ash, J. Hazard.

Mater. 162 (2009) 812–818. doi:10.1016/j.jhazmat.2008.05.125.

[9] K.J. Hong, S. Tokunaga, T. Kajiuchi, Extraction of heavy metals from MSW incinerator fly ashes by chelating agents, J. Hazard. Mater. 75 (2000) 57–73. doi:10.1016/S0304-3894(00)00171-0.

[10] L. Zheng, C. Wang, W. Wang, Y. Shi, X. Gao, Immobilization of MSWI fly ash through geopolymerization: Effects of water-wash, Waste Manag. 31 (2011) 311–317. doi:10.1016/j.wasman.2010.05.015.

[11] H.Y. Wu, Y.P. Ting, Metal extraction from municipal solid waste (MSW) incinerator fly ash - Chemical leaching and fungal bioleaching, Enzyme Microb. Technol. 38 (2006) 839–847. doi:10.1016/j.enzmictec.2005.08.012.

[12] W.S. Chen, F.C. Chang, Y.H. Shen, M.S. Tsai, C.H. Ko, Removal of chloride from MSWI fly ash, J. Hazard. Mater. 237–238 (2012) 116–120. doi:10.1016/j.jhazmat.2012.08.010.

[13] F. Colangelo, R. Cioffi, F. Montagnaro, L. Santoro, Soluble salt removal from MSWI fly ash and its stabilization for safer disposal and recovery as road basement material, Waste Manag. 32 (2012) 1179–1185. doi:10.1016/j.wasman.2011.12.013.

[14] X. Wang, A. Li, Z. Zhang, The Effects of Water Washing on Cement-based Stabilization of MWSI Fly Ash, Procedia Environ. Sci. 31 (2016) 440–446. doi:10.1016/j.proenv.2016.02.095.

[15] Y. Yang, Y. Xiao, J.H.L. Voncken, N. Wilson, Thermal treatment and vitrification of boiler ash from a municipal solid waste incinerator, J. Hazard. Mater. 154 (2008) 871–879. doi:10.1016/j.jhazmat.2007.10.116.

[16] K.Y. Chiang, Y.H. Hu, Water washing effects on metals emission reduction during municipal solid waste incinerator (MSWI) fly ash melting process, Waste Manag. 30 (2010) 831–838. doi:10.1016/j.wasman.2009.12.009.

[17] M. Aguiar del Toro, W. Calmano, H. Ecke, Wet extraction of heavy metals and chloride from MSWI and straw combustion fly ashes, Waste Manag. 29 (2009) 2494–2499. doi:10.1016/j.wasman.2009.04.013.

[18] T. Mangialardi, Disposal of MSWI fly ash through a combined washing-immobilisation process, J. Hazard. Mater. 98 (2003) 225–240. doi:10.1016/S0304-3894(02)00359-X.

[19] C. Fernández Pereira, Y. Luna, X. Querol, D. Antenucci, J. Vale, Waste stabilization/solidification of an electric arc furnace dust using fly ash-based geopolymers, Fuel. 88 (2009) 1185–1193. doi:10.1016/j.fuel.2008.01.021.

[20] P. Duxson, A. Fernández-Jiménez, J.L. Provis, G.C. Lukey, A. Palomo, J.S.J. Van Deventer, Geopolymer technology: The current state of the art, J. Mater. Sci. 42 (2007) 2917–2933. doi:10.1007/s10853-006-0637-z.

[21] W.D.A. Rickard, J. Temuujin, A. Van Riessen, Thermal analysis of geopolymer pastes synthesised from five fly ashes of variable composition, J. Non. Cryst. Solids. 358 (2012) 1830–1839. doi:10.1016/j.jnoncrysol.2012.05.032.

[22] I. Phummiphan, S. Horpibulsuk, R. Rachan, A. Arulrajah, S.L. Shen, P. Chindaprasirt, High calcium fly ash geopolymer stabilized lateritic soil and granulated blast furnace slag blends as a pavement base material, J. Hazard. Mater. 341 (2018) 257–267. doi:10.1016/j.jhazmat.2017.07.067.

[23] J. Temuujin, A. van Riessen, Effect of fly ash preliminary calcination on the properties of geopolymer, J. Hazard. Mater. 164 (2009) 634–639. doi:10.1016/j.jhazmat.2008.08.065.

[24] J. Temuujin, A. Van Riessen, K.J.D. MacKenzie, Preparation and characterisation of fly ash based geopolymer mortars, Constr. Build. Mater. 24 (2010) 1906–1910. doi:10.1016/j.conbuildmat.2010.04.012.

[25] D. Khale, R. Chaudhary, Mechanism of geopolymerization and factors influencing its development: A review, J. Mater. Sci. 42 (2007) 729–746. doi:10.1007/s10853-006-0401-4.

[26] Y. Luna Galiano, C. Fernández Pereira, J. Vale, Stabilization/solidification of a municipal solid waste incineration residue using fly ash-based geopolymers, J. Hazard. Mater. 185 (2011) 373–381. doi:10.1016/j.jhazmat.2010.08.127.

[27] Y. Yahaya, J. Zhou, D. Ping, Z. Shu, Yun Chen, Effects of pH dynamics on solidification/stabilization of municipal solid waste incineration fly ash, J. Environ.

Manage. 207 (2018) 243–248. doi:10.1016/j.jenvman.2017.11.042.

[28] Y. Yakubu, J. Zhou, Z. Shu, Y. Zhang, W. Wang, Y. Mbululo, Potential application of pre-treated municipal solid waste incineration fly ash as cement supplement, Environ. Sci. Pollut. Res. (2018). doi:10.1007/s11356-018-1851-3.

[29] K. Shiota, T. Nakamura, M. Takaoka, S.F. Aminuddin, K. Oshita, T. Fujimori, Stabilization of lead in an alkali-activated municipal solid waste incineration fly ash–Pyrophyllite-based system, J. Environ. Manage. 201 (2017) 327–334. doi:10.1016/j.jenvman.2017.07.002.

[30] L. Zheng, W. Wang, X. Gao, Solidification and immobilization of MSWI fly ash through aluminate geopolymerization: Based on partial charge model analysis, Waste Manag. 58 (2016) 270–279. doi:10.1016/j.wasman.2016.08.019.

[31] M. Jin, Z. Zheng, Y. Sun, L. Chen, Z. Jin, Resistance of metakaolin-MSWI fly ash based geopolymer to acid and alkaline environments, J. Non. Cryst. Solids. 450 (2016) 116–122. doi:10.1016/j.jnoncrysol.2016.07.036.

[32] X. Guo, W. Hu, H. Shi, Microstructure and self-solidification/stabilization (S/S) of heavy metals of nano-modified CFA-MSWIFA composite geopolymers, Constr. Build. Mater. 56 (2014) 81–86. doi:10.1016/j.conbuildmat.2014.01.062.

[33] X. Gao, W. Wang, T. Ye, F. Wang, Y. Lan, Utilization of washed MSWI fly ash as partial cement substitute with the addition of dithiocarbamic chelate, J. Environ. Manage. 88 (2008) 293–299. doi:10.1016/j.jenvman.2007.02.008.

[34] L. Faming, Y. Shujin, M. Jie, Mechanical Properties of Concrete After Chlorine Salt Extraction in Freeze-Thaw Environment, (2014) 360–367.